EL SEVIER

#### Contents lists available at ScienceDirect

# Ultramicroscopy

journal homepage: www.elsevier.com/locate/ultramic



# Beam-sensitive metal-organic framework structure determination by microcrystal electron diffraction



Fateme Banihashemi<sup>a,1</sup>, Guanhong Bu<sup>a,b,1</sup>, Amar Thaker<sup>a,b</sup>, Dewight Williams<sup>c</sup>, Jerry Y.S. Lin<sup>a</sup>, Brent L. Nannenga<sup>a,b,\*</sup>

- <sup>a</sup> Chemical Engineering, School for Engineering of Matter, Transport and Energy, Arizona State University, 501 E. Tyler Mall, PO Box 876106, Tempe, AZ 85287, United States
- b Biodesign Center for Applied Structural Discovery, Biodesign Institute, Arizona State University, 727 East Tyler Street, Tempe, AZ 85287, United States
- <sup>c</sup> John M. Cowley Center for High Resolution Electron Microscopy, Arizona State University, Tempe, AZ, United States

#### ARTICLE INFO

# Keywords: Metal-organic framework Microcrystal electron diffraction Crystallography CryoEM MicroED Electron diffraction

## ABSTRACT

Analysis of metal-organic framework (MOF) structure by electron microscopy and electron diffraction offers an alternative to growing large single crystals for high-resolution X-ray diffraction. However, many MOFs are electron beam-sensitive, which can make structural analysis using high-resolution electron microscopy difficult. In this work we use the microcrystal electron diffraction (MicroED) method to collect high-resolution electron diffraction data from a model beam-sensitive MOF, ZIF-8. The diffraction data could be used to determine the structure of ZIF-8 to 0.87 Å from a single ZIF-8 nanocrystal, and this refined structure compares well with previously published structures of ZIF-8 determined by X-ray crystallography. This demonstrates that MicroED can be a valuable tool for the analysis of beam-sensitive MOF structures directly from nano and microcrystalline material

# 1. Introduction

Metal-organic frameworks represent a new class of microporous materials. Zeolitic imidazolate frameworks (ZIFs) are a subcategory of highly crystalline MOF materials bearing zeolitic topologies finding wide variety of applications in adsorption, separation, gas storage, and heterogeneous catalysis. ZIF-8 with sodalite (SOD) topology has been among the most extensively studied ZIF materials [1, 2]. Many MOF structures are determined by single crystal X-ray diffraction [3], however this requires the growth of large crystals to withstand the effects of radiation damage and allow the collection of sufficient diffraction data. In some cases, powder diffraction data alone can be used for structure determination; however, this can be a more difficult approach. Because MOFs are often synthesized as micro and nanocrystals, the use of transmission electron microscopy offers a way to study the MOF structure directly from the synthesized material. Collecting data at cryogenic temperatures improves data collection from beam-sensitivity MOFs, and this can be further improved by using low dose imaging conditions (in the range of 4 – 12  $e^{-}/\text{Å}^{2}$  total exposure) and direct electron detection [4-7]. Imaging thin sections of MOF fragments provides an excellent approach for directly visualizing interfacial, surface,

and local structure of these beam sensitive materials.

As an alternative to imaging based TEM structure determination methods for overall structure determination, electron diffraction can also be employed for high-resolution structure determination from crystalline materials, including MOFs [8-11]. In recent years, electron microscopy methods, such as microcrystal electron diffraction (MicroED) [12, 13], have been employed to determine the structures of a variety of samples from various fields including materials science, organic chemistry, and structural biology [12-18]. A key benefit of electron diffraction is that crystals several orders of magnitude smaller than those used for single crystal X-ray methods can be used for high-resolution structure determination, which bypasses the often times difficult and time-consuming steps of growing large single crystals for structural analysis.

As is the case with imaging, very low electron dose must be used when beam-sensitive materials are being analyzed by electron diffraction. MicroED is a technique that uses ultra-low dose to collect electron diffraction data at cryogenic temperature from very small microcrystals as the stage continually rotates [12, 13, 19]. By using sufficiently low dose and continuous rotation of the sample, large volumes of reciprocal space can be sampled before the crystal is overcome by radiation

<sup>\*</sup> Corresponding author.

E-mail address: Brent.Nannenga@asu.edu (B.L. Nannenga).

<sup>&</sup>lt;sup>1</sup> These authors contributed equally to this work

damage [20, 21], which allows for the indexing and integration of the diffraction data set. MicroED has been successfully applied to many samples including proteins, peptides, small molecules, and natural products [22-32].

In this work, we make use of ZIF-8 as a model beam-sensitive MOF [5] and demonstrate that MicroED data collection procedures are suitable for rapid structure determination of these materials at very high-resolution. The ZIF-8 MicroED data were collected and processed using a cryo-TEM equipped with a high-speed camera for diffraction data collection, and did not require any other specialized hardware. The ZIF-8 data from a single crystal were processed to 0.87 Å and an *ab initio* structure was determined, which compares well to previously solved structures of ZIF-8 determined by single crystal X-ray crystallography.

#### 2. Methods

## 2.1. ZIF-8 synthesis

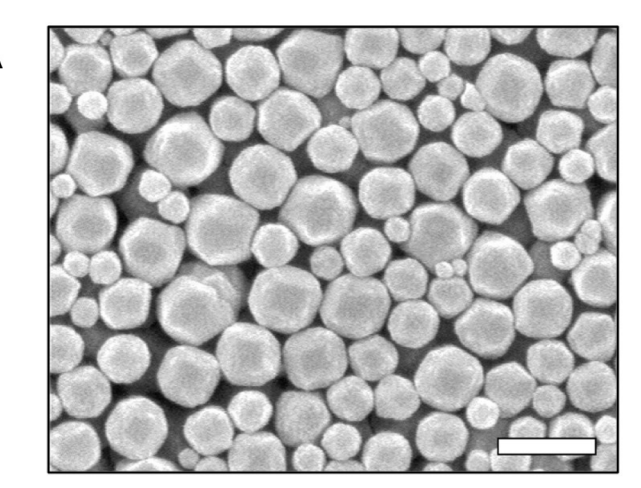
ZIF-8 crystals were synthesized by modifying the procedure reported by Tanaka and co-workers [33]. All chemicals were purchased from Sigma-Aldrich (U.S.A) unless otherwise stated. Zinc nitrate hexahydrate [ $Zn(NO_3)$ .6 $H_2O$ ] (98%, 0.297 g) was dissolved in 20 ml of deionized water and 3.28 g of 2-methylimidazole (MeIM) was dissolved separately in 20 ml of deionized water. The separate dissolved solutions were stirred for 10 min. The imidazole solution was poured into the zinc solution and stirred for 1 h. The solution quickly became cloudy and a suspension was obtained. The final molar composition of the synthesis solution was Zn<sup>+</sup>: MeIM: Water = 1: 40: 2227. After mixing, the resultant white solution was centrifuged at 5000 g for 10 min and washed with methanol (VWR, 99.8%) 3 times. The Products were then dried overnight in vacuum oven at room temperature. The morphology and crystallographic properties of ZIF-8 crystals was examined using scanning electron microscope (SEM, Amray 1910) and X-ray powder diffraction (XRD, AXS-D8, Bruker) with a scan step of 0.015° using Cu Kα radiation (λ = 1.543 Å), respectively.

# 2.2. MicroED ZIF-8 sample preparation

Dried, lightly ground ZIF-8 crystals (0.004 g) were placed in a glass vial containing 100 ml of methanol to form 0.005 wt.% colloidal ZIF-8 solution. 2  $\mu$ L of prepared solution were applied onto the surface of glow-discharged Quantifoil 300-mesh 2/2 grids, and dried by evaporation for a few minutes. Grids were subsequently placed into autoloader cartridges under liquid nitrogen and loaded into a Titan Krios cryo-TEM (Thermo Fisher Scientific) operated at 300 kV and equipped with a CETA D detector (Thermo Fisher Scientific), which was used for diffraction data collection.

# 2.3. MicroED data collection

MicroED data were collected using similar protocols described previously [19, 34]. Low-dose settings for the Titan Krios cryo-TEM were employed throughout screening and data collection steps. Crystals that were well-separated from other crystals on the grid were identified using low magnification search mode. Upon the identification of single microcrystals suitable for data collection, initial diffraction patterns were collected by switching the microscope into diffraction mode using the pre-calibrated and aligned "exposure mode" within the low dose settings. If a high quality diffraction pattern was obtained, the microscope was put back into search mode and the maximal tilt range of for data collection (i.e. the range where crystal remained centered and no other crystals or grid bars moved into the path of the beam) was determined. The stage was tilted to the maximum angle and the selected area aperture and beam stop were inserted. The selected area aperture size was selected such that the entire crystal was within the aperture while also minimizing the area surrounding the crystal. MicroED data



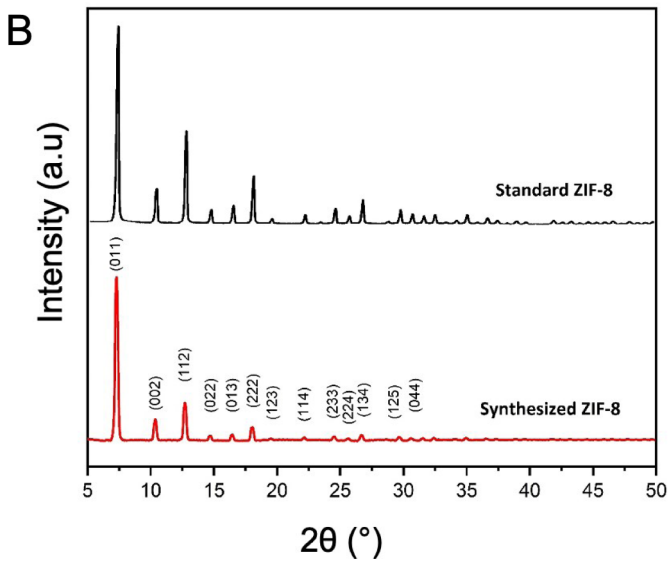


Fig. 1. (A) SEM micrograph of synthesized ZIF-8 and (B) XRD powder diffraction data of standard [41] and synthesized ZIF-8 crystals. Scale bar in A represents 1  $\mu m$ .

sets were collected by continuously rotating the crystal (0.7° per second) in the beam as the CETA D camera was continuously acquiring diffraction frames at a rate of 2 s per frame. The exposure rate was approximately  $0.02~e^-/\text{Å}^2$  per frame.

# 2.4. Data processing and structure determination

Diffraction data sets were converted to SMV format [35] and indexed, integrated and scaled using XDS [36]. The structure of ZIF-8 was ultimately determined with data from a single crystal by direct methods using SHELXT [37] followed by refinement using the ShelXle interface [38].

# 3. Results and discussion

The morphology of the synthesized ZIF-8 crystals were observed by SEM as shown in Fig. 1A. ZIF-8 crystals shows an approximate isotropic hexagon envelope with particle size range of 200 to 800 nm. The XRD powder diffraction pattern from prepared ZIF-8, is consistent with that of standard ZIF-8 samples reported in literature [39-41] (Fig. 1B), thus revealing the successful synthesis of ZIF-8. The as-synthesized ZIF-8 particles were suspended in methanol, and this solution was directly deposited on a holey carbon coated EM grid. Following the evaporation of the methanol from the surface of the grid, the EM grid was loaded

0.8 Å

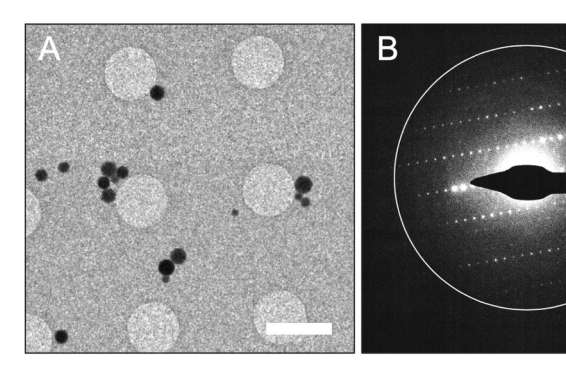


**Fig. 2.** ZIF-8 crystals yield high resolution diffraction patterns. (A) A low magnification search of the EM grid shows well-dispersed ZIF-8 crystals on the surface of the holey-carbon. (B) Electron diffraction pattern collected from a high-quality ZIF-8 nanocrystal shows sharp and well-separated spots extending to high-resolution. This diffraction pattern represents what was typically seen for crystals which were used for MicroED data collection. Scale bar in A represents 3 µm.

into the Titan Krios cryo-TEM and the ZIF-8 particle distribution was assessed. The distribution of particles is important for MicroED because individual crystals need to be isolated for data collection to ensure that data from multiple crystals is not collected. When viewed at lower magnification, it can be seen that while many of the ZIF-8 nanoparticles preferred to clump together, there were a significant fraction of particles that were well-dispersed and amenable to data collection (Fig. 2A).

ZIF-8 crystals ranging in diameter from approximately 200 nm to 800 nm could be seen on the grids. While screening crystal quality by taking initial diffraction patterns from each crystal, it was found that the diffraction data became qualitatively worse (i.e. lower resolution and more background noise from the increased diffuse scattering) as the size of the ZIF-8 nanoparticles approached the larger end of the size range (approximately 400 nm to 800 nm in diameter). The crystals which were on the smaller end of the size range (approximately 200 nm to 400 nm in diameter), generally produced better diffraction, and crystals that produced the data with the highest resolution and sharpest diffraction spots were used for data collection (Fig. 2B). Ultimately, the crystal that produced the data used for structure determination was approximately 200 nm across and 200 nm thick. This is significantly smaller than the size of crystals used for single crystal X-ray methods which have dimensions on the order of tens to hundreds of micrometers.

In a previous study, it was demonstrated that ZIF-8 samples rapidly lose their crystallinity in the electron beam [5]. Therefore, the total exposure for each crystal during the course of MicroED data collection was kept to  $\sim 1 e^{-}/\text{Å}^2$ , which is much lower than the what was used the recent high-resolution imaging studies of ZIF-8 particles [4, 5, 7]. The time to collect a MicroED data set is relatively short (in the range of 1 to 2 min for the ZIF-8 samples), and because many of the ZIF-8 nanocrystals in the 200 to 400 nm size range diffracted to beyond 1 Å, we could specifically focus on crystals of this size. This allowed the collection of many high-resolution data sets in a short amount of time. With sample loading, microscope setup, crystal screening for only the best crystals, and data collection are all taken into account, we collected 12 high-quality data sets in approximately 2 h. The ability to rapidly collect a large number of data sets is a great advantage for the use of MicroED in the study of MOFs and other organic, biological, or beamsensitive crystalline samples.

While data from many crystals were collected, because of the high symmetry of the ZIF-8 nanocrystals, data from a single crystal could ultimately be used for structure determination to 0.87 Å (Table 1). When processed, data from one single crystal resulted in a data set that

**Table 1**Data collection and refinement statistics

	ZIF-8
Data collection	_
Excitation Voltage	300 kV
Wavelength (Å)	0.019687
Number of crystals	1
Data Processing	
Space group	I-43m
Unit cell length $a = b = c  (\mathring{A})$	16.880
Angles $\alpha = \beta = \gamma$ (°)	90.00
Resolution (Å)	8.45 - 0.87
Number of reflections	7466
Unique reflections	407
R <sub>obs</sub> (%)	34.3 (159.0)
R <sub>meas</sub> (%)	35.8 (163.3)
$I/\sigma_I$	4.37 (1.11)
CC <sub>1/2</sub> (%)	97.2 (57.0)
Completeness (%)	99.8 (100.0)
Structure Refinement	
R1	0.1779
wR2	0.3411
GooF	1.011

Values in parentheses represent numbers in the highest resolution shell (1.02 – 0.87 Å).

was 99.8% complete. It should be noted that many other crystals in the data sets collected could also be used for structure determination as well. The direct methods solution found was in space group I-43 m and 5 atoms were placed within the asymmetric unit, which is what would be expected for ZIF-8. Following structure refinement (R1 = 0.1779, wR2 = 0.3411, and GooF = 1.011) and expanding the asymmetric unit, the structure of ZIF-8 can be seen, with each zinc being coordinated by 4 MeIM ligands and each ligand bridges 2 zinc atoms (Fig. 3). This produces the typical SOD zeolite type structure with hex-zinc-atomic open ring channels of 3.4 Å in diameter. Both the unit cell parameters and atom positions of the MicroED structure compare well with previous ZIF-8 structures determined by single crystal X-ray diffraction [39, 42, 43], with differences in bond lengths between the MicroED structures and the X-ray structures being in the range of 0.03 to 0.07 Å.

### Conclusion

The accurate determination MOF structure is critical to understanding and engineering the properties of these materials, and it is important to make use of methods capable of facilitating the rapid determination of beam-sensitive MOFs. The cryo-EM method of MicroED is a fast and reliable method for structure determination from micro and nanocrystals, and we have shown here that this procedure can be easily extended to the ab initio structure determination and analysis of beam sensitive MOFs. A benefit of the MicroED method is that it can be performed on many of the same cryo-TEM instruments used for high-resolution imaging. Future combinations of MicroED structure determination with low-dose high-resolution imaging could allow multi-leveled analysis of beam-sensitive materials from a single sample, where diffraction is used for high-resolution structure determination and the images can analyze surface and interfacial structure. This would further establish low-dose cryo-TEM as an invaluable tool for understanding MOF structure and function.

# Data availability

Coordinates for ZIF-8 have been deposited in the Cambridge Structural Database (CCDC 1997958)

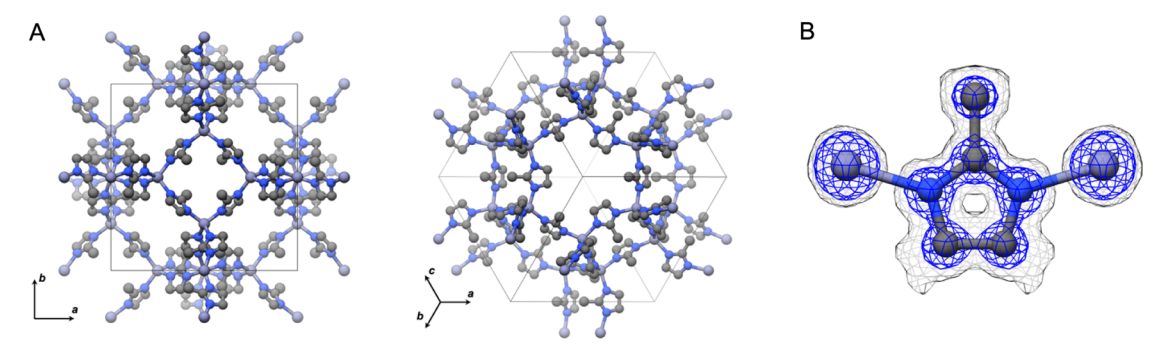


Fig. 3. MicroED structure and unit cell of ZIF-8 viewed in different orientations (A) and the surrounding density (B). The maps in panel B are contoured at  $0.8\sigma$  (gray) and  $2.4\sigma$  (blue). Hydrogens are omitted from the figures for clarity.

#### Acknowledgement

FB and JYSL would like to acknowledge support from the National Science Foundation (CBET-1511005). BLN would like acknowledge the support from the National Science Foundation (DMR-1942084) and the National Institutes of Health (R21GM135784). We would like to acknowledge the use of the Titan Krios at the Eyring Materials Center at Arizona State University and the funding of this instrument by NSF MRI 1531991.

#### **Declaration of Competing Interest**

The authors declare that they have no known competing financial interests or personal relationships that could have appeared to influence the work reported in this paper.

#### References

- C. Zhang, R.P. Lively, K. Zhang, J.R. Johnson, O. Karvan, W.J. Koros, Unexpected molecular sieving properties of zeolitic imidazolate framework-8, J. Phys. Chem. Lett. 3 (2012) 2130–2134.
- [2] Z. Zhao, Z. Li, Y.S. Lin, Adsorption and diffusion of carbon dioxide on metal organic framework (MOF-5), Ind. Eng. Chem. Res. 48 (2009) 10015–10020.
- [3] F. Gandara, T.D. Bennett, Crystallography of metal-organic frameworks, IUCrJ 1 (2014) 563–570.
- [4] Y. Li, K. Wang, W. Zhou, Y. Li, R. Vila, W. Huang, H. Wang, G. Chen, G.-H. Wu, Y. Tsao, H. Wang, R. Sinclair, W. Chiu, Y. Cui, Cryo-EM structures of atomic surfaces and host-guest chemistry in metal-organic frameworks, Matter 1 (2019) 429, 429.
- [5] Y.H. Zhu, J. Ciston, B. Zheng, X.H. Miao, C. Czarnik, Y.C. Pan, R. Sougrat, Z.P. Lai, C.E. Hsiung, K.X. Yao, I. Pinnau, M. Pan, Y. Han, Unravelling surface and interfacial structures of a metal-organic framework by transmission electron microscopy, Nat. Mater. 16 (2017) 532.
- [6] X. Li, J. Wang, X. Liu, L. Liu, D. Cha, X. Zheng, A.A. Yousef, K. Song, Y. Zhu, D. Zhang, Y. Han, Direct imaging of tunable crystal surface structures of MOF MIL-101 using high-resolution electron microscopy, J. Am. Chem. Soc. 141 (2019) 12021–12028.
- [7] D. Zhang, Y. Zhu, L. Liu, X. Ying, C.-.E. Hsiung, R. Sougrat, K. Li, Y. Han, Atomic-resolution transmission electron microscopy of electron beam–sensitive crystalline materials, Science (2018) eaao0865.
- [8] L. Zhu, D. Zhang, M. Xue, H. Li, S. Qiu, Direct observations of the MOF (UiO-66) structure by transmission electron microscopy, Cryst. Eng. Comm. 15 (2013) 9356–9359.
- [9] M. Feyand, E. Mugnaioli, F. Vermoortele, B. Bueken, J.M. Dieterich, T. Reimer, U. Kolb, D. de Vos, N. Stock, Automated diffraction tomography for the structure elucidation of twinned, sub-micrometer crystals of a highly porous, catalytically active bismuth metal-organic framework, Angew. Chem. Int. Ed. 51 (2012) 10373–10376.
- [10] S. Yuan, J.-.S. Qin, H.-.Q. Xu, J. Su, D. Rossi, Y. Chen, L. Zhang, C. Lollar, Q. Wang, H.-.L. Jiang, D.H. Son, H. Xu, Z. Huang, X. Zou, H.-.C. Zhou, [Ti8Zr2O12(COO)16] Cluster: an ideal inorganic building unit for photoactive metal-organic frameworks, ACS Cent. Sci. 4 (2018) 105–111.
- [11] D. Denysenko, M. Grzywa, M. Tonigold, B. Streppel, I. Krkljus, M. Hirscher, E. Mugnaioli, U. Kolb, J. Hanss, D. Volkmer, Elucidating gating effects for hydrogen sorption in MFU-4-type triazolate-based metal-organic frameworks featuring different pore sizes, Chemistry (Easton) 17 (2011) 1837–1848.
- [12] B.L. Nannenga, MicroED methodology and development, Struct. Dyn. 7 (2020) 014304.
- [13] B.L. Nannenga, T. Gonen, The cryo-EM method microcrystal electron diffraction (MicroED), Nat. Methods 16 (2019) 369–379.

- [14] M. Gemmi, E. Mugnaioli, T.E. Gorelik, U. Kolb, L. Palatinus, P. Boullay,
  S. Hovmöller, J.P. Abrahams, 3D Electron Diffraction: The Nanocrystallography
  Revolution, ACS Central Science, 2019.
  [15] T. Gruene, J.T.C. Wennmacher, C. Zaubitzer, J.J. Holstein, J. Heidler, A. Fecteau-
- [15] T. Gruene, J.T.C. Wennmacher, C. Zaubitzer, J.J. Holstein, J. Heidler, A. Fecteau-Lefebvre, S. De Carlo, E. Muller, K.N. Goldie, I. Regeni, T. Li, G. Santiso-Quinones, G. Steinfeld, S. Handschin, E. van Genderen, J.A. van Bokhoven, G.H. Clever, R. Pantelic, Rapid structure determination of microcrystalline molecular compounds using electron diffraction, Angew. Chem. Int. Ed. Engl. 57 (2018) 16313–16317.
- [16] C.G. Jones, M.W. Martynowycz, J. Hattne, T.J. Fulton, B.M. Stoltz, J.A. Rodriguez, H.M. Nelson, T. Gonen, The CryoEM method MicroED as a powerful tool for small molecule structure determination, ACS Cent. Sci. 4 (2018) 1587–1592.
- [17] P. Brázda, L. Palatinus, M. Babor, Electron diffraction determines molecular absolute configuration in a pharmaceutical nanocrystal, Science 364 (2019) 667.
- [18] L. Palatinus, P. Brazda, P. Boullay, O. Perez, M. Klementova, S. Petit, V. Eigner, M. Zaarour, S. Mintova, Hydrogen positions in single nanocrystals revealed by electron diffraction, Science 355 (2017) 166–169.
- [19] B.L. Nannenga, D. Shi, A.G. Leslie, T. Gonen, High-resolution structure determination by continuous-rotation data collection in MicroED, Nat. Methods 11 (2014) 927-930
- [20] J. Hattne, D. Shi, C. Glynn, C.T. Zee, M. Gallagher-Jones, M.W. Martynowycz, J.A. Rodriguez, T. Gonen, Analysis of global and site-specific radiation damage in cryo-EM, Structure 26 (2018) 759–766 e754.
- [21] D. Shi, B.L. Nannenga, M.G. Iadanza, T. Gonen, Three-dimensional electron crystallography of protein microcrystals, Elife 2 (2013) e01345.
- [22] R.A. Warmack, D.R. Boyer, C.-T. Zee, L.S. Richards, M.R. Sawaya, D. Cascio, T. Gonen, D.S. Eisenberg, S.G. Clarke, Structure of amyloid-β (20-34) with Alzheimer's-associated isomerization at Asp23 reveals a distinct protofilament interface, Nat. Commun. 10 (2019) 3357.
- [23] C.P. Ting, M.A. Funk, S.L. Halaby, Z. Zhang, T. Gonen, W.A. van der Donk, Use of a scaffold peptide in the biosynthesis of amino acid-derived natural products, Science 365 (2019) 280.
- [24] M.D. Purdy, D. Shi, J. Chrustowicz, J. Hattne, T. Gonen, M. Yeager, MicroED structures of HIV-1 Gag CTD-SP1 reveal binding interactions with the maturation inhibitor bevirimat, Proceedings of the National Academy of Sciences, 2018 201806806.
- [25] P. Krotee, S.L. Griner, M.R. Sawaya, D. Cascio, J.A. Rodriguez, D. Shi, S. Philipp, K. Murray, L. Saelices, J. Lee, P. Seidler, C.G. Glabe, L. Jiang, T. Gonen, D.S. Eisenberg, Common fibrillar spines of amyloid-beta and human islet amyloid polypeptide revealed by microelectron diffraction and structure-based inhibitors, J. Biol. Chem. 293 (2018) 2888–2902.
- [26] M. Gallagher-Jones, C. Glynn, D.R. Boyer, M.W. Martynowycz, E. Hernandez, J. Miao, C.T. Zee, I.V. Novikova, L. Goldschmidt, H.T. McFarlane, G.F. Helguera, J.E. Evans, M.R. Sawaya, D. Cascio, D.S. Eisenberg, T. Gonen, J.A. Rodriguez, Subangstrom cryo-EM structure of a prion protofibril reveals a polar clasp, Nat. Struct. Mol. Biol. 25 (2018) 131–134.
- [27] M.R. Sawaya, J. Rodriguez, D. Cascio, M.J. Collazo, D. Shi, F.E. Reyes, J. Hattne, T. Gonen, D.S. Eisenberg, Ab initio structure determination from prion nanocrystals at atomic resolution by MicroED, Proc. Natl. Acad. Sci. U S A (2016).
- [28] B.L. Nannenga, D. Shi, J. Hattne, F.E. Reyes, T. Gonen, Structure of catalase determined by MicroED, Elife 3 (2014) e03600.
- [29] M. Dick, N.S. Sarai, M.W. Martynowycz, T. Gonen, F.H. Arnold, Tailoring tryptophan synthase TrpB for selective quaternary carbon bond formation, J. Am. Chem. Soc. 141 (2019) 19817–19822.
- [30] J.A. Rodriguez, M.I. Ivanova, M.R. Sawaya, D. Cascio, F.E. Reyes, D. Shi, S. Sangwan, E.L. Guenther, L.M. Johnson, M. Zhang, L. Jiang, M.A. Arbing, B.L. Nannenga, J. Hattne, J. Whitelegge, A.S. Brewster, M. Messerschmidt, S. Boutet, N.K. Sauter, T. Gonen, D.S. Eisenberg, Structure of the toxic core of alphasynuclein from invisible crystals, Nature (2015).
- [31] H. Xu, H. Lebrette, M.T.B. Clabbers, J. Zhao, J.J. Griese, X. Zou, M. Högbom, Solving a new R2lox protein structure by microcrystal electron diffraction, Sci. Adv. 5 (2019) eaax4621.
- [32] A.M. Levine, G. Bu, S. Biswas, E.H.R. Tsai, A.B. Braunschweig, B.L. Nannenga, Crystal structure and orientation of organic semiconductor thin films by microcrystal electron diffraction and grazing-incidence wide-angle X-ray scattering, Chem. Commun. 56 (2020) 4204–4207.

[33] K. Kida, M. Okita, K. Fujita, S. Tanaka, Y. Miyake, Formation of high crystalline ZIF-8 in an aqueous solution, Cryst. Eng. Comm. 15 (2013) 1794–1801.

- [34] D. Shi, B.L. Nannenga, M.J. de la Cruz, J. Liu, S. Sawtelle, G. Calero, F.E. Reyes, J. Hattne, T. Gonen, The collection of MicroED data for macromolecular crystallography, Nat Protoc 11 (2016) 895–904.
- [35] J. Hattne, F.E. Reyes, B.L. Nannenga, D. Shi, M.J. de la Cruz, A.G. Leslie, T Gonen, MicroED data collection and processing, Acta Crystallogr. A Found. Adv. 71 (2015) 353–360.
- [36] W. Kabsch, Xds, Acta Crystallogr. D Biol. Crystallogr. 66 (2010) 125-132.
- [37] G.M. Sheldrick, SHELXT integrated space-group and crystal-structure determination, Acta Crystallogr. A Found Adv. 71 (2015) 3–8.
- [38] C.B. Hubschle, G.M. Sheldrick, B. Dittrich, ShelXle: a Qt graphical user interface for SHELXL, J. Appl. Crystallogr. 44 (2011) 1281–1284.
- [39] K.S. Park, Z. Ni, A.P. Côté, J.Y. Choi, R. Huang, F.J. Uribe-Romo, H.K. Chae, M. O'Keeffe, O.M. Yaghi, Exceptional chemical and thermal stability of zeolitic

- imidazolate frameworks, Proceed. Natl. Acad. Sci. 103 (2006) 10186–10191. [40] G. Liu, Z. Jiang, K. Cao, S. Nair, X. Cheng, J. Zhao, H. Gomaa, H. Wu, F. Pan,
- [40] G. Liu, Z. Jiang, K. Cao, S. Nair, X. Cheng, J. Zhao, H. Gomaa, H. Wu, F. Pan, Pervaporation performance comparison of hybrid membranes filled with two-dimensional ZIF-L nanosheets and zero-dimensional ZIF-8 nanoparticles, J. Memb. Sci. 523 (2017) 185–196.
- [41] G. Liu, Y. Xu, Y. Han, J. Wu, J. Xu, H. Meng, X. Zhang, Immobilization of lysozyme proteins on a hierarchical zeolitic imidazolate framework (ZIF-8), Dalton Trans. 46 (2017) 2114–2121.
- [42] W. Morris, C.J. Stevens, R.E. Taylor, C. Dybowski, O.M. Yaghi, M.A. Garcia-Garibay, NMR and X-ray study revealing the rigidity of zeolitic imidazolate frameworks, J. Phys. Chem. C 116 (2012) 13307–13312.
- [43] H.T. Kwon, H.-.K. Jeong, A.S. Lee, H.S. An, J.S. Lee, Heteroepitaxially grown zeolitic imidazolate framework membranes with unprecedented propylene/propane separation performances, J. Am. Chem. Soc. 137 (2015) 12304–12311.